

Synthesis of Silver Nanoparticles Using *Azadirachta indica* Leaf Extracts for Heavy Metal Sensing

Abidemi Mercy Babatimehin,^{a,b,*} Gabriel Olukayode Ajayi,^c Oyebola Elizabeth Ogunbamowo,^{a,d} Ali El-Rayyes,^e Lamia A. Albedair,^f Amnah Mohammed Alsuhaibani,^g and Edwin Andrew Ofudje^a

Silver nanoparticles (AgNPs) were synthesized *via* a cheap bio-reduction and green method from leaf extracts of *Azadirachta indica*. The technique was optimized for variables such as pH, temperature, and concentration of the plant extracts. Gas chromatography mass spectroscopy (GC-MS) results indicated the presence of phytonutrients, such as piperidine, 2-azacyclooctanone, 4-dibenzofuranamine, lauric anhydride, cyclododecanol, and sorbic acid as the phytonutrients responsible for the reduction and resilience process. Fourier transform infrared results gave absorption bands indicating the presence of -OH, -NH, and -C=O functional groups, while particle size analysis revealed an average particle size that is less than 100 nm, thus confirming the formation of a nanoparticle. Ultraviolet-visible investigation of the nanoparticles synthesized with concentration of 12.5 mg/mL produced a strong plasmon resonance band with an absorbance of 0.223 at 400 nm after 24 h incubation time. At a minimal concentration of 6.25 mg/mL, the absorbance further decreased with a bathochromic shift to 600 nm. The synthesized AgNPs showed excellent optical property towards the selected heavy metals with color change and a shift in absorbance towards higher value. Selective detection of Pb²⁺, Cu²⁺, and Cd²⁺ was also confirmed by UV-visible spectra, which is well noticed with Pb²⁺ having the highest absorbance.

DOI: 10.15376/biores.20.2.3342-3366

Keywords: *Azadirachta indica*; Optimization; Optical sensor; Heavy metals; Nanoparticles

Contact information: a: Department of Chemical Science, Mountain Top University, Lagos- Ibadan Expressway, Move, Ogun State, Nigeria; b: Department of Biochemistry, Lagos State University, Ojo, Lagos, Nigeria; c: Department of Biochemistry, Mountain Top University, Lagos - Ibadan Expressway, Move, Ogun state, Nigeria; d: Department of Medical Biochemistry, Lagos State University College of Medicine, Ikeja, Lagos, Nigeria; e: Center for Scientific Research and Entrepreneurship, Northern Border University, Arar 73213, Saudi Arabia; f: Department of Chemistry, College of Science, Princess Nourah bint Abdulrahman University, P.O. Box 84428, Riyadh 11671, Saudi Arabia; g: Department of Sports Health, College of Sport Sciences & Physical Activity, Princess Nourah bint Abdulrahman University, P.O. Box 84428, Riyadh 11671, Saudi Arabia;

* Corresponding author: abidemibabatimehin530@gmail.com

INTRODUCTION

Elements with atomic density greater than 5 g/cm³ are known as heavy metals (HM). These include Cd, Ag, Co, Fe, Cr, Cu, Hg, Zn, Pb, Zn, As, and Pt-group elements and they could either be toxic or essential for living organisms (Babel and Kurniawan 2003; Fu and Wang 2015; Zwolak *et al.* 2019). The agrarian and industrial revolutions, coupled with rapid increase in population, has led to increasing demands for resources

from businesses, and this high industrial productivity has resulted in increasing generation of effluents such as HM and other toxins (Zwolak *et al.* 2019). This has far-reaching consequences for the receiving ecosystems and their valuable resources. As a result, toxic metal pollution has consistently degraded the ecosystem, reducing its ability to support life and provide fundamental supports (Akinwekomi *et al.* 2017; Magagane *et al.* 2019). Heavy metals (HMs) have been linked to genotoxic, mutagenic, teratogenic, and carcinogenic effects, making them hazardous to living organisms (Liao *et al.* 2016; Hills *et al.* 2019). While some HMs are essential for biological processes, excessive exposure can damage cells and tissues, with lead, mercury, and cadmium being particularly toxic, leading to severe health conditions such as mental retardation and organ toxicity (Hou *et al.* 2013; Sun *et al.* 2015; Kaji 2015; Mitra *et al.* 2016; Jayamurali *et al.* 2021). Industrial activities, such as mining, metal smelting, manufacturing, and chemical processing contribute significantly to heavy metal pollution, which is often a point source of contamination (Ali *et al.* 2013; Badhiwala *et al.* 2015). Non-point source pollution, caused by agricultural and urban activities, is harder to control due to its dispersed nature and diverse contaminants (Tabassum *et al.* 2017). Additionally, natural weathering processes can contribute to environmental pollution, making heavy metal management complex despite their biological importance (Wang *et al.* 2015; Vareda *et al.* 2019).

It is vital to precisely identify heavy metal concentrations to reduce their presence in the environment and alleviate the conditions of soil and water resources (Duodu *et al.* 2016). Several techniques for detecting HMs ions have been reported, which include Inductively coupled plasma mass spectrometry (ICP-MS) and inductively coupled plasma optical emission spectrometry (ICP-OES) (Duodu *et al.* 2016), Atomic absorption spectroscopy (AAS) and flameless atomic absorption spectrophotometry (FAAS) are all used in the detection of heavy metals (Daşbaşı *et al.* 2016). These processes are highly responsive and discerning approaches; nonetheless, each of them necessitates the use of relatively expensive instruments, complex operational processes, and extended detection periods that often limit their usage (Daşbaşı *et al.* 2016).

Nanotechnology (nanotech) is becoming prominent in technology and is regularly regarded as a novel industrial innovation dealing with materials in the range 1.0 to 100 nm in length (Nasrollahzadeh *et al.* 2019). The principles of nanotech are founded on the notion that the properties of materials vary as the dimensions are reduced to the nano scale (Singh *et al.* 2020). Nanoscience, a newly emerging subject, gives a potential to filter water with low cost, high efficacy in detecting and removing pollutants, and a good reusability (Baruah *et al.* 2016). The approved green and environmentally acceptable method for nanoparticles (NPs) synthesis uses biological materials such as green plants and microorganisms. Plants are widely available. Various metabolites consisting of pharmacological components could serve as green-reducing agents in the production of NPs (Singh *et al.* 2020). Experts have discovered that nanomaterials are a superior option for detecting pollutants in effluent, as they have characteristic features that can include large surface area, high solution mobility, minute size, and high reactivity (Wu *et al.* 2019). Some of them possess high porosity, dispersibility, hydrophilicity, strong mechanical properties, and hydrophobicity (Yaqoob and Ibrahim 2019). Moreover, the chemical synthesis of nanomaterials (NMs) comes with several disadvantages, which include the utilization of reducing agents and the adsorption of hazardous chemicals on the NPs' surface, which might have negative consequences in their applications. As an alternative, synthesis of NPs *via* green approach has garnered great interest because of its

environmentally friendly technique (Dhand *et al.* 2016; Jebril *et al.* 2020). Metallic NPs' distance-dependent optical and different size behavior make them ideal for sensing HMs ions in polluted water (Ahmed and Mustafa 2020). Scientists have explored the potential applications of metal oxide/metal NPs synthesized using extracts of plants leaf (Annadhasan *et al.* 2014). Metal NPs colorimetric application is a function of the size of the nanomaterial that could be obtained through optimization of the synthetic conditions.

The primary mechanisms involved include surface plasmon resonance (SPR), nanoparticle aggregation, complex formation, and redox reactions. SPR occurs when conduction electrons on metallic nanoparticles oscillate in response to incident light, leading to strong absorption and scattering. When metal ions bind to nanoparticles, they induce a shift in the SPR band, which can be monitored spectroscopically to detect specific ions (Alberti *et al.* 2021). Nanoparticle aggregation further enhances metal ion sensing. For instance, dispersed gold nanoparticles (AuNPs) exhibit a red color due to their SPR peak at around 520 nm (Du *et al.* 2012). However, interactions with certain metal ions can induce aggregation, altering the SPR properties and causing a visible color change, such as red to blue or purple. Similarly, complex formation occurs when nanoparticles functionalized with specific ligands bind to metal ions, leading to optical or electrochemical changes, as in the case of AgNPs complexing with lead ions (Pb^{2+}), resulting in a color shift from dark brown to light brown due to aggregation (Du *et al.* 2012). Redox reactions also play a role in nanoparticle-based metal ion detection. Some metal ions undergo oxidation or reduction when interacting with nanoparticles, altering the nanoparticles' morphology and SPR properties (Maity *et al.* 2018). This can lead to a measurable color change, as seen when iron(III) ions (Fe^{3+}) react with AgNPs, causing a red shift in the SPR band (Maity *et al.* 2018). Overall, these mechanisms of SPR shifts, aggregation-induced color changes, complex formation, and redox reactions enable highly sensitive and selective detection of metal ions using nanoparticles.

The exceptional opto-electronic characteristics coupled with tiny surface properties of silver nanoparticles (AgNPs) have made its sensing application even at low detection limits feasible, which is a unique feature. Similarly, the toxicity caused to the environment by the usage of chemicals as reducing and stabilizing agents as well as the cost of purchasing chemicals have been reduced with the adoption of a green synthesis method, which necessitated this current study. Neem (*Azadirachta indica*) is widely used in the synthesis of silver nanoparticles (AgNPs) due to its rich composition of bioactive compounds. The plant contains flavonoids, tannins, terpenoids, and alkaloids, which act as natural reducing and stabilizing agents. These phytochemicals facilitate the conversion of silver ions (Ag^+) into silver nanoparticles (Ag^0) without the need for toxic chemical reagents, making the synthesis process safer and more sustainable (Kumari *et al.* 2022; Bhat1 *et al.* 2019). In addition to being eco-friendly and cost-effective, neem-mediated synthesis eliminates hazardous chemicals commonly used in conventional nanoparticle production (Kumari *et al.* 2022; Bhat1 *et al.* 2019). The presence of phytochemicals such as proteins, polysaccharides, and phenolic compounds in neem extracts have been reported to help cap and stabilize AgNPs, preventing aggregation and ensuring long-term stability; this property enhances the efficiency and reliability of AgNP applications, particularly in medicine and environmental science (Kumari *et al.* 2022; Bhat1 *et al.* 2019).

This study aimed to synthesize silver nanoparticles (AgNPs) using *Azadirachta indica* (neem) leaf extract through a green, cost-effective, and eco-friendly method. To enhance the synthesis process, key parameters such as pH, temperature, and plant extract

concentration were optimized. The synthesized AgNPs were then characterized using UV-Vis spectroscopy, Fourier transform infrared (FTIR), X-ray diffraction (XRD), and scanning electron microscopy/ energy dispersive X-ray (SEM/EDX) analysis to confirm their structural, optical, and morphological properties. Their optical behavior, particularly surface plasmon resonance (SPR), was investigated to assess their potential as optical sensors. Furthermore, the AgNPs were evaluated for their ability to detect heavy metal ions, including Pb^{2+} , Cu^{2+} , and Cd^{2+} , through observable colorimetric changes and shifts in absorption spectra. A selectivity study was also conducted to determine which metal ions induced the most significant response, highlighting the potential application of these biosynthesized AgNPs in heavy metal sensing.

EXPERIMENTAL

Materials

Reagents used, such as $PbCl_2$, $CuSO_4$, $FeSO_4$, $NaCl$, $LiCl$, Cl_2 , and $CdCl_2$, were of high purity and were purchased from Sigma Aldrich in Cape Town, South Africa. All glassware was cleaned with distilled and deionized water and dried in an oven.

Extract from Plant Source Preparation

Leaves of *Azadirachta indica* (Neem) were collected from a matured tree within Lagos State University Zoological Garden, Nigeria (GPS N-06° 28.214 E-003 11.864). The authentication of the plant species was done by subject experts at the Botany Department, Lagos State University, Nigeria. The collected leaves were cleaned many times using distilled water to remove dirt and were dried at room temperature for 10 days. Each of the samples was reduced into smaller sizes and pulverized into its powdery form. A total of 5 g of the powdered *Azadirachta indica* was soaked in 100 mL of H_2O for 24 h. Subsequently, the mixture was sieved, and the obtained extract solution was kept and thereafter used for nanoparticle synthesis.

Phytochemical Analysis of Plant Extract

The plant extract above was analyzed using GC-MS analysis to examine the phytochemicals available in the plant extract using 7820 A gas chromatography coupled to 5975C inert mass spectrometer and electron impact source (Agilent Technologies). Scanning of potential phytochemicals was done at 2.62 s/scan rate within m/z 30 to 550 amu.

Qualitative analysis

The qualitative assessment of phytonutrients in neem leaf extract was conducted following the methodology outlined by Mudhafar *et al.* (2020).

Alkaloids test

Wagner's reagent (iodine in potassium iodide) was added to the extract. The formation of a reddish-brown precipitate confirmed the presence of alkaloids.

Flavonoids test

A few drops of sodium hydroxide (NaOH) solution were introduced into the extract. A yellow coloration that faded upon adding a dilute acid indicated the presence of flavonoids.

Phenols test

The extract was treated with a few drops of ferric chloride (FeCl₃) solution. A blue-green or violet color indicated the presence of phenols.

Saponins test

The extract was vigorously shaken with distilled water. The formation of stable foam confirmed the presence of saponins.

Tannins test

A gelatin solution was added to the extract. The formation of a white precipitate signified the presence of tannins.

Terpenoids test

The extract was combined with chloroform and concentrated sulfuric acid (H₂SO₄). A reddish-brown coloration at the interface indicated the presence of terpenoids.

Quantitative analysis

The quantitative determination of phytonutrients was carried out using spectrophotometric methods.

Total phenolic content (TPC)

The Folin-Ciocalteu reagent was used to determine TPC. The extract was mixed with the reagent and sodium carbonate (Na₂CO₃), and absorbance was recorded at 765 nm.

Total flavonoid content (TFC)

The aluminum chloride (AlCl₃) method was used for flavonoid quantification. The extract was mixed with AlCl₃ solution, and absorbance was measured at 510 nm.

Total alkaloid content (TAC)

Determination of alkaloids was performed using the bromocresol green (BCG) method. The extract was mixed with BCG solution, and absorbance was measured at 470 nm.

Total saponin content (TSC)

The vanillin-sulfuric acid method was employed for saponin quantification. The extract was treated with vanillin reagent and sulfuric acid, and absorbance was measured at 544 nm.

Total terpenoid content (TTC)

The extract was mixed with chloroform and sulfuric acid, and total terpenoid content was determined by measuring absorbance at 538 nm, with linalool as the standard.

Silver Nanoparticles Synthesis

The preparation was done by adopting the method described by Ahmed and Mustafa (2020) but modified using sustainable green method with no toxic capping or reducing agents. 100 mL of 1 mM silver nitrate salt were added to 10 mL of plant extracts stock solutions with increasing concentrations of the plant extract (0.2 to 50 mg/L) and incubated at varying temperatures (25 to 100 °C) and placed on a shaker at 120 rpm. After 1 h of shaking, absorbance was taken using a UV-Vis spectrophotometer (SM 7504, Shanghai, China) ranging from 300 to 600 nm. This same method was repeated using different values of pH (2.0, 4.0, 6.0, 8.0, and 10.0), temperature (30, 40, 50, 70, and 100 °C), and plant extract concentration (100, 50, 25, 12.5, and 6.25 mg/mL).

Characterization

The UV-Visible spectrophotometer (SM 7504, Shanghai, China) was utilized to characterize and sense the prepared AgNPs.

The shapes of the produced AgNPs powders were studied using a scanning electron microscope (SEM) equipped with a Hitachi (Japan) S-3000H electron microscope operating at 15 kV.

The chemical analysis of the produced AgNPs powders was determined using the equipped EDX.

The X-ray crystallography of the AgNPs were conducted with a Rigaku Miniflex machine. This was done to study the crystalline features of the AgNPs produced at the range of $2\theta = 10^\circ$ to 70° .

Particle size distribution of the prepared AgNPs was investigated using Nanotrack coupled with Microtrap FLEX 10.5.2 software.

The FTIR analysis for both the neem leaf and synthesized AgNPs was performed using Thermo Fisher Scientific Instrument model CARY630 NBY. The KBr pellet approach was used, which involved mixing of the synthesized AgNPs powder and KBr in a mortar and pestle and compressing it to produce a 2 mm diameter pellet. All FTIR spectra data were obtained in the region of 400 to 4000 cm^{-1} at a resolution of 4 cm^{-1} and 64 times scanning.

Metal Ions Recognition Ability of the AgNPs Synthesized from Neem Leaf Extract

The synthesized AgNPs were used to sense metals in water by the method described by Koduru *et al.* (2018). 1.0 mL of the prepared nanoparticles was combined with 1.0 mL solution of 100 μM metal salts (NaCl, PbCl_2 , FeSO_4 , CuSO_4 , CdCl_2 , ZnCl_2 , NiCl_2) at 35 °C, and the colorimetric responses and absorption intensity changes was checked using UV-VIS spectroscopy at the wavelength range of 300 to 600 nm. The readings were taken in duplicate and the average value recorded for a period of 24 hrs.

RESULTS AND DISCUSSION

Neem Leaf Phytochemical Analysis

Preliminary tests were carried out to determine qualitatively and quantitatively the phytochemicals present in the plant extract and the results obtained are presented in Tables 1 and 2.

Azadirachta indica (AI) leaf extract was screened for phytoconstituents. It was found that the aqueous extract contained different secondary metabolites, including sugars, amino acids, triterpenes, and phenols with the absence of phlebotomine, which is in line with the report of Dash *et al.* (2017) as depicted in Table 1. Table 2 displays quantitative screening results for alkaloids, flavonoids, terpenoids, and saponins in the leaf of *Azadirachta indica*.

The highest percentage was noticed with tannin (90.3 mg/mL), followed by flavonoids (64.9 mg/mL), phenol (61.6 mg/mL), reducing sugar (49.8 mg/mL), cardiac glycoside (27.8 mg/mg), alkaloid (8.29 mg/mL), while the least value was observed with saponin (7.82 mg/mL). The presence of such compounds is responsible for the reduction of Ag^+ to Ag^0 , and the compounds can also function as capping and stabilizing factors for green produced AgNPs (Raja *et al.* 2014; Choi *et al.* 2018). Plant-based capping agents may be responsible for the stability of AgNPs in solution, as no indication of agglomeration was seen 6 h after their synthesis.

Table 1. Qualitative Analysis of Neem Leaf Extract

	Tannin	Phenol	Phlebotomine	Alkaloid	Saponin	Flavonoid	Steroid	Anthraquinone	Terpenoid	Cardiac glycoside	Reducing sugar
Leaf	+	+	-	+	+	+	+	+	+	+	+

Table 2. Quantitative Analysis of Neem Leaf Extract (mg/mL)

	Tannin	Phenol	Saponin	Alkaloid	Reducing Sugar	Cardiac Glycoside	Flavonoid
Leaf (mg/mL)	90.32	61.65	7.82	8.29	49.81	27.77	64.88

GC-MS Analysis

The GC-MS of the neem leaf extract is represented in Fig. 1, which depicts the mass spectra, while the bioactive compounds with their molecular formulae, retention time (RT), peak area (%), and structures are shown in Table 3. The fragmentation patterns of the mass spectra were matched to those of recognized compounds from the National Institute of Standards and Technology (NIST) research collection, Nigeria. Results show the presence of tridecane, 4-dibenzofuranamine, dodecane, 5-iodononane, dodecanoic acid, dodecanoyl chloride, 2-azacyclooctanone, 2,5-dimethyl-5-ethyl-4,5-dihydro-1,3-oxazole, cyclododecanol 1-aminomethyl, and many more.

The compounds identified through GC-MS analysis play vital roles in the synthesis and functionality of AgNPs. Phenolics, alkaloids, terpenoids, and fatty acids act as reducing agents, facilitating Ag^+ reduction, while flavonoids, aromatic compounds, and fatty acids serve as capping and stabilizing agents, preventing nanoparticle aggregation (Koduru *et al.* 2018; Ahmed *et al.* 2020).

Furthermore, the functional groups present in these compounds enable the AgNPs to act as effective colorimetric sensors for detecting heavy metal ions (Annadhasan *et al.*

2014). These multifunctional properties make neem leaf extract an excellent natural source for green nanoparticle synthesis with potential applications in environmental monitoring and biomedicine.

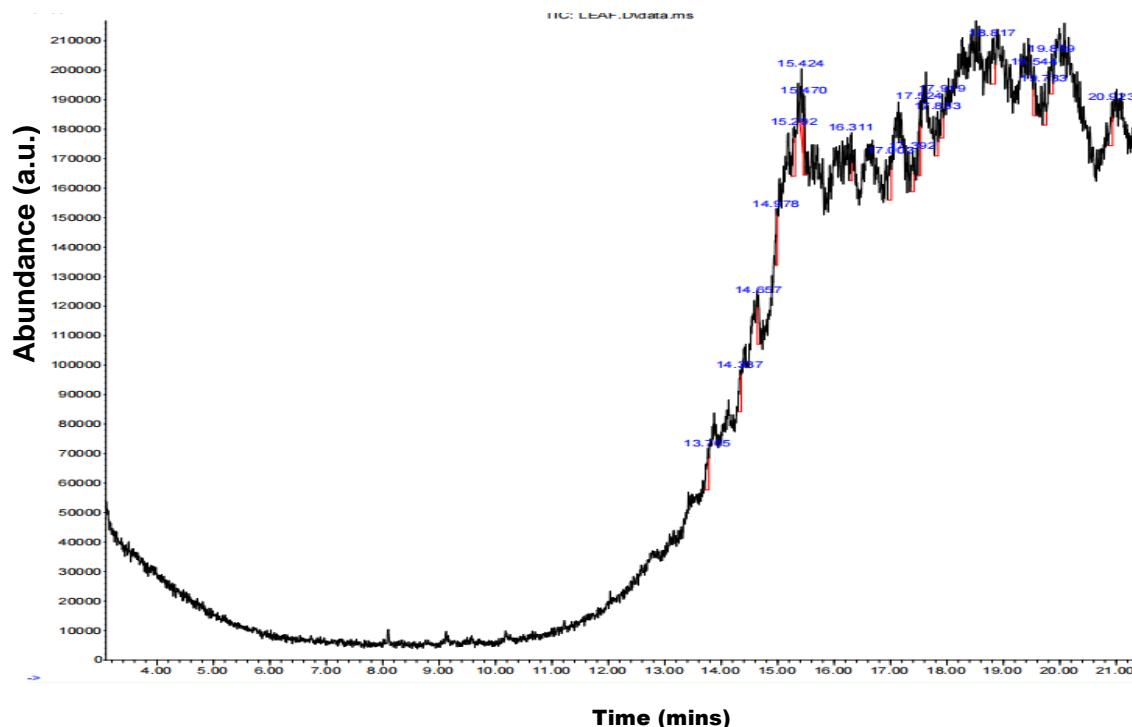
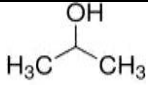
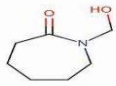
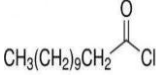
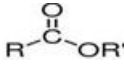
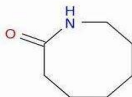
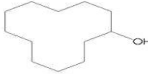
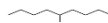
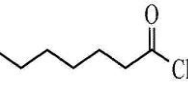
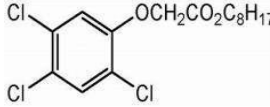
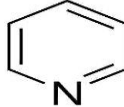



Fig. 1. GC-MS of neem leaf extract

Table 3. GC-MS Analysis of Neem Leaf Extract Indicating Retention Time (RT)

RT	% Area	Compounds	Structures
13.76	10.31	Tridecane	
14.33	9.45	Fumaric acid	
14.657	10.31	Carbonic acid	
14.97	9.22	Dodecane	
15.292	11.55	Myristic acid	
15.670	10.62	Sorbic acid	
16.311	10.62	Myristoyl chloride	
16.47	10.62	Cyclododecanol	

17.00	11.87	2- Propanol	
17.329	12.35	2H-Azepin-2-one	
17.52	12.94	Dodecanoyl chloride	
17.83	14.36	Ethenyl ester	
17.833	9.36	2-Azacyclooctanone	
17.919	13.24	Cyclododecanol	
18.81	14.67	5-Iodo nonane	
19.544	14.73	Octanoyl chloride	
19.733	14.67	Isooctyl ester	
19.859	14.82	Pyridine	
20.923	14.66	N-Ethyl-hexahydro-1H-azepine	

Silver Nanoparticles Preparation

The formation of silver nanoparticles (AgNPs) was visually confirmed by a noticeable color change in the reaction mixture appearing golden yellow to golden brown within 60 min indicating the production of AgNPs (Shankar *et al.* 2004). After about 60 min, the reaction mixture's color changed completely and did not change again. This shows that all the possible reduction had been achieved, and that the reducing ability still remained in excess. According to Krishnaraj *et al.* (2010), *Acalypha indica* leaf extract contains compounds, such as caffeine and theophylline, that function as reducing agents. However, in neem leaves extract, natural reducing agents include the presence of terpenoids, flavanones, among others, which reduces silver salt to AgNPs. According to Shankar *et al.* (2004), the yellowish-brown color of AgNPs in aqueous solution is due to

the surface plasmon vibrations. The main sign of AgNPs formation is because of the change in color from gold to dark brown as indicated in Fig. 2.



Fig. 2. Different color change indicating neem leaf extract (NM), neem leaf extract with AgNO_3 after 1.0 h (NL1), and after 6 h (NL2)

Characterizations

The AgNPs formed was determined by obtaining their absorption spectra using UV-Vis spectroscopic techniques (Fig. 3). Silver nanoparticles have unique optical characteristics that generate strong interactions with distinctive wavelengths of light. In AgNPs, electrons travel easily due to a minimal difference between the valence and conduction bands, and these free electrons generate a surface plasmon resonance (SPR) absorption band. The SPR band is formed when AgNPs collectively oscillate, and electrons resonate with light waves (Krishnaraj *et al.* 2010). The measurement of the UV-Vis spectra confirmed the formation of the AgNPs with maximum absorbance between 350 nm and 400 nm (Fig. 3), with higher energy levels as were achieved by Shankar *et al.* (2004) and Khalil *et al.* (2014) using olive leaves. The SEM/EDX analyses were used to assess the morphology and elemental compositions in the newly produced nanoparticles. The SEM examination revealed that most of AgNPs consist of agglomerated small particles (Fig. 4), while the EDX (Fig. 5) spectra of AgNPs synthesized from neem leaf extract verified the presence of elemental silver in the sample in addition to other elements. The presence of carbon is likely from the organic compounds present in neem leaf extract, while the identification of oxygen suggests the presence of oxygen-containing functional groups, such as phenolics and flavonoids, which may play a role in reducing and stabilizing AgNPs. The presence of N could be from proteins and alkaloids involved in the capping process, while the detection of silver confirms the formation of silver nanoparticles. Silicon, phosphorus, potassium, magnesium, and aluminum were present in minor quantities, possibly originating from the neem extract or as environmental contaminants. The AgNPs synthesized were characterized using XRD to establish their crystal structure. Figure 6 shows three distinct XRD peaks of AgNPs at 38.8° (111), 45.0° (200), and 65.2° (220) as observed for the AgNPs synthesized (Ahmed and Mustafa 2020). Only single-phase nanoparticles were formed.

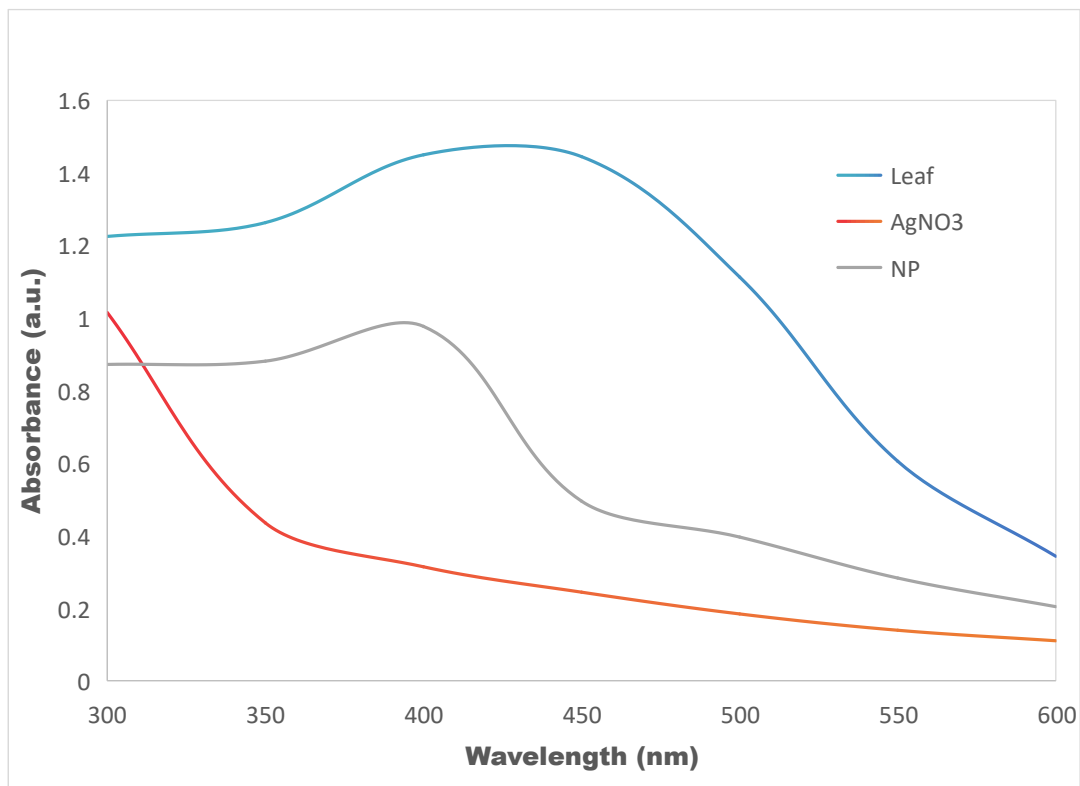


Fig. 3. UV-Vis spectra of: Leaf = neem leaf extract alone, AgNO₃ = silver nitrate solution alone, and NP = synthesized AgNPs

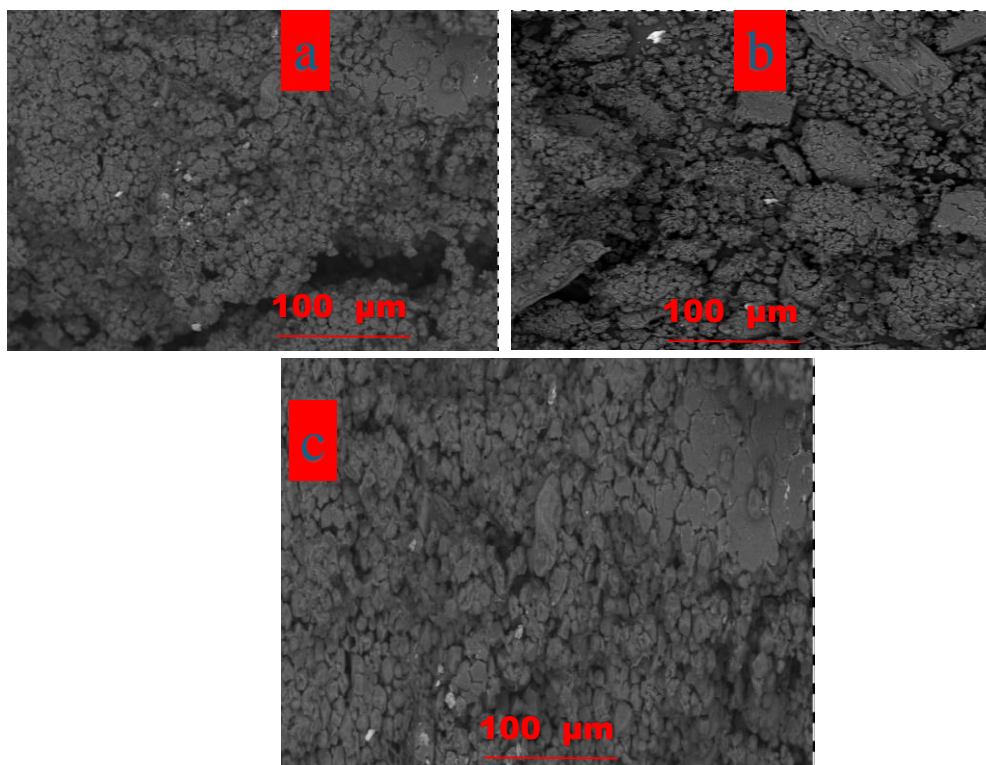


Fig. 4. SEM of AgNPs synthesized at (a) 100 mg/mL, (b) 50 mg/mL, and (c) 25 mg/mL of the neem leaf extract

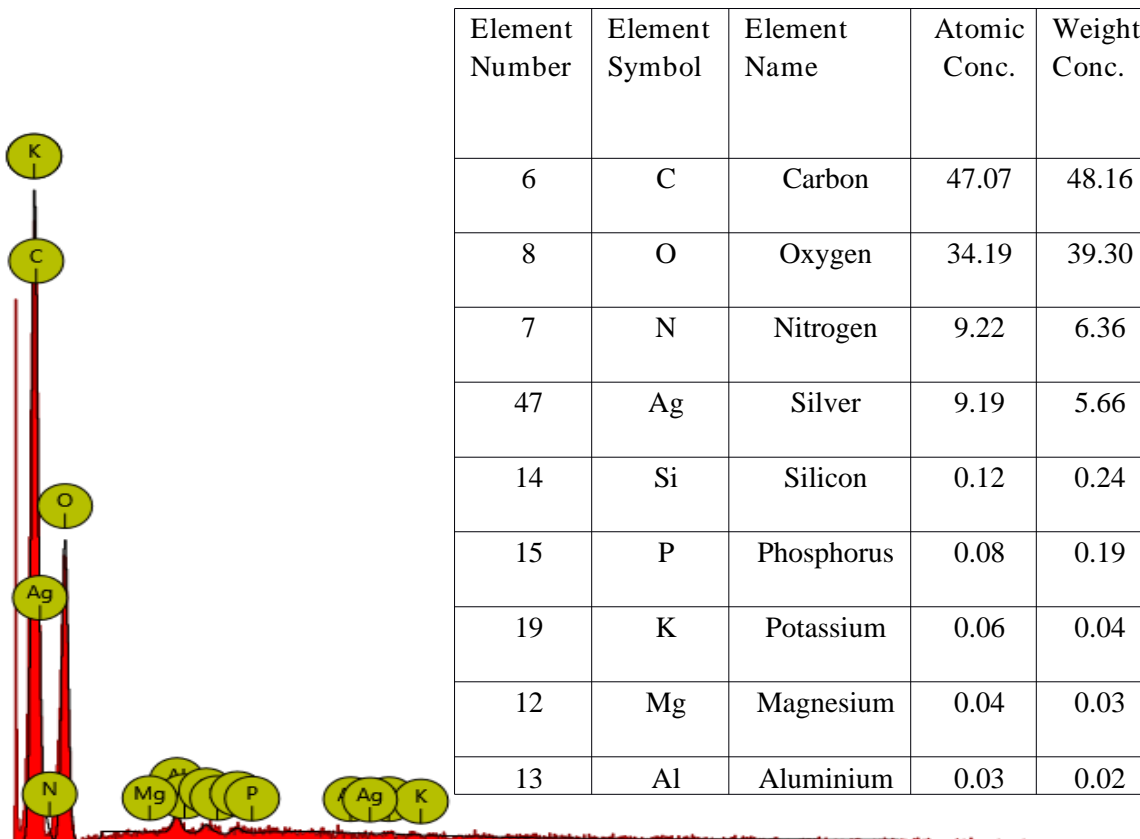


Fig. 5. EDX analysis of the synthesized AgNPs at 50 mg/mL of the neem extract

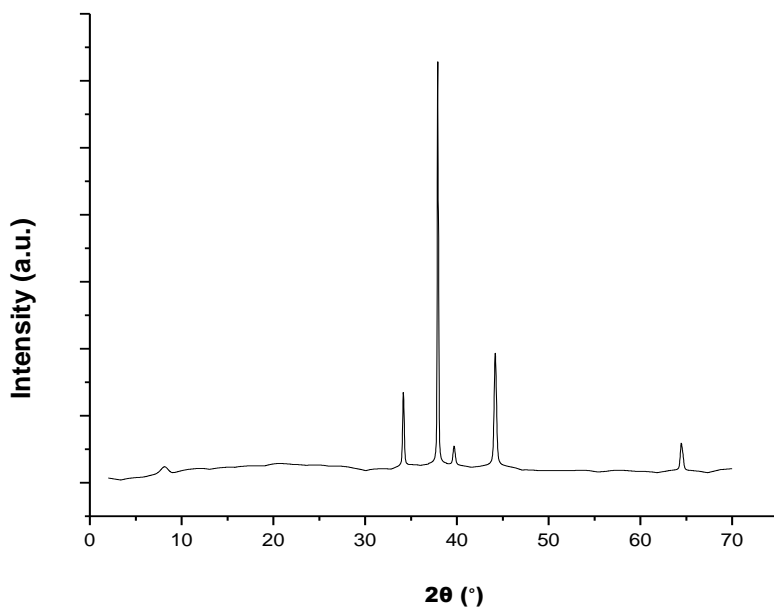


Fig. 6. XRD spectrum of AgNPs at 50 mg/mL of the neem extract

Figures 7 to 9 reveals the particle size investigation of the synthesized AgNPs at 100 mg/mL (Fig. 7), 50 mg/mL (Fig. 8), and 25 mg/mL (Fig. 9) of the neem extract. The size distribution shows that the synthesized AgNPs were 81.5 nm synthesized at 100 mg/mL of the extract, whereas the particle size distributions of the AgNPs produced from 50 and 25 mg/mL of the plant extract showed bimodal distributions of 0.52 and 66.2 nm and 0.73 and 39.7 nm, respectively. The particle size increased when the plant extract concentration increased, as reduced particle size distribution indicates the formation of a nanosized material at smaller concentration of the neem extract.

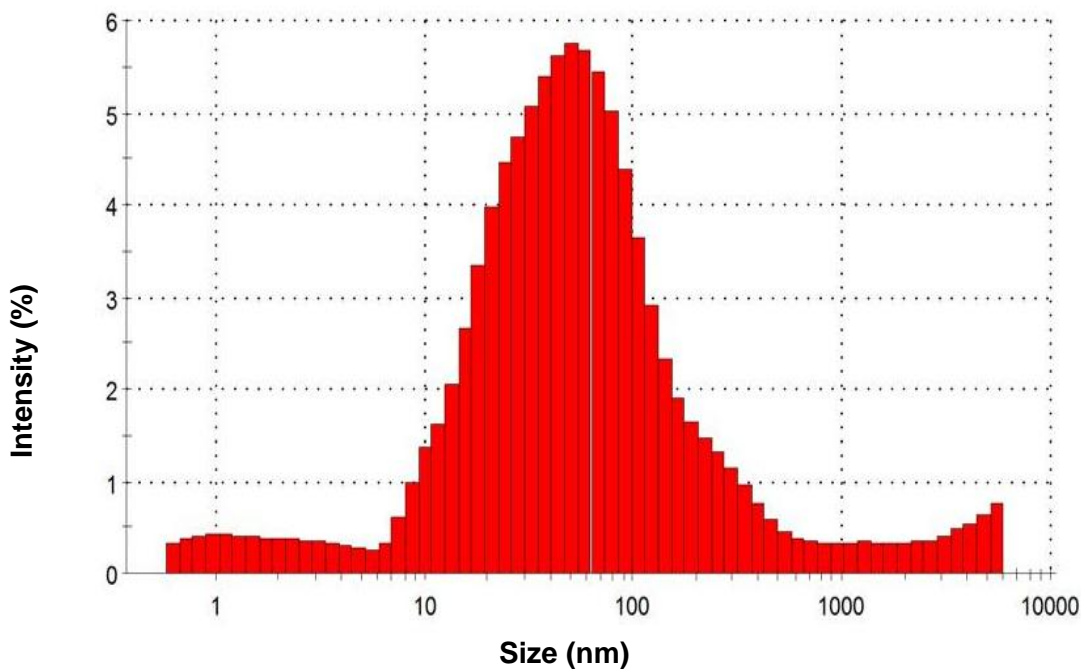


Fig. 7. Particle size of synthesized AgNPs at 100 mg/mL of the neem extract

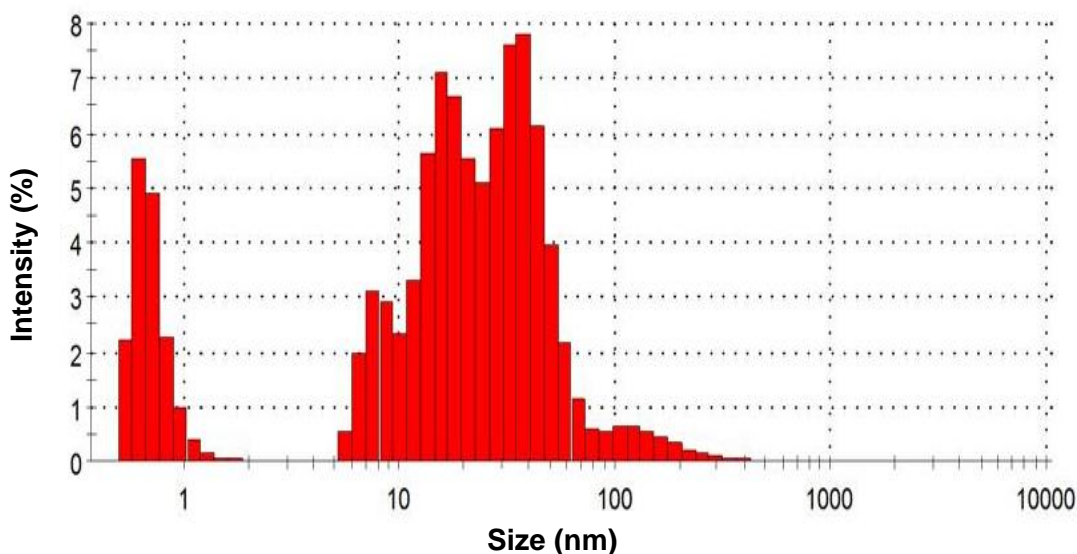


Fig. 8. Particle size of synthesized AgNPs at 50 mg/mL of the neem extract

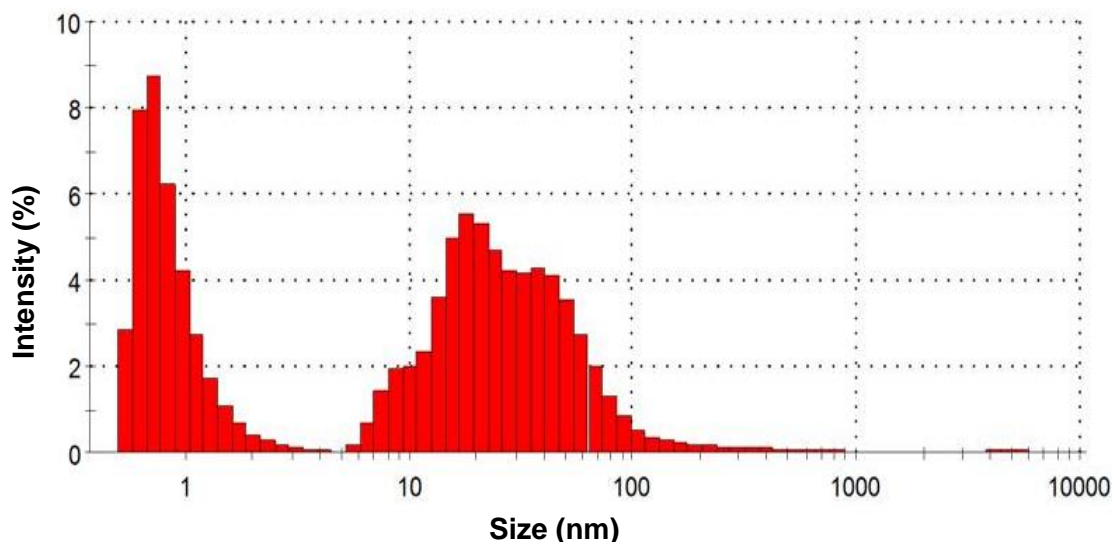


Fig. 9. Particle size of synthesized AgNPs at 25 mg/mL of the neem extract

The FTIR spectroscopy was used in identifying the functional groups meant for reducing and stabilizing AgNPs, which confirms the existence of several biomolecules in the leaf extract and their conjugation with silver (Fig. 10a and b). The absorption spectra for both neem extract and synthesized AgNPs show phenol ring and nitrosamine, with a prominent band at 1457.4 and 1450.2 cm^{-1} , respectively (Velusamy *et al.* 2015). Hydroxyl compounds were identified by the presence of bands at 3462.7 and 3480.2 cm^{-1} for the extract and nanoparticle, respectively. In neem leaf extract, the amine N-H bending vibration overlapped with the phenolic groups -OH stretching band, which resulted in a significant stretching band at 3462 cm^{-1} . The phenol -OH groups have been reported to reduce Ag^+ to Ag^0 (Meenambal *et al.* 2012). When the neem leaf extract was mixed with AgNO_3 solution, it weakened the strength of the peak at 3462.7 cm^{-1} , thus indicating that neem's carboxylic acids also caused the reduction reaction (Meenambal *et al.* 2012; Velusamy *et al.* 2015). The FTIR spectra show a peak at 1647 cm^{-1} , indicating C=O bands of carboxylic acid in the extract. Previous investigations have shown that C=O-C and C=O groups can act as stabilizing agents in the green synthesis of nanomaterials (Meenambal *et al.* 2012). The bands at 2967.0 and 2855.1 cm^{-1} were identified as cycloalkanes, whereas the band located at 1580.4 cm^{-1} was caused by the presence of a phenol ring. The spectra of AgNPs produced by neem leaf extract (Fig. 10b) showed a sharp peak at 3480.2 cm^{-1} for -OH of phenolic groups and 1602.1 cm^{-1} for N-H amine (bend). The disappearance or shift in peak's positions in the FTIR spectra of AgNPs clearly support the participation of these groups in the reduction process of Ag^+ to Ag^0 and as stabilizing agent. The availability of -OH in the extract enables the stabilization of the AgNPs, which could be related to reduction in the capping agent of the plant extract. In this current study, the FTIR analysis revealed the participation of phenol, amines, carboxylic acids, and nitrosamine in the synthesis of AgNPs, which is an agreement with previous reported in literature (Raja *et al.* 2014).

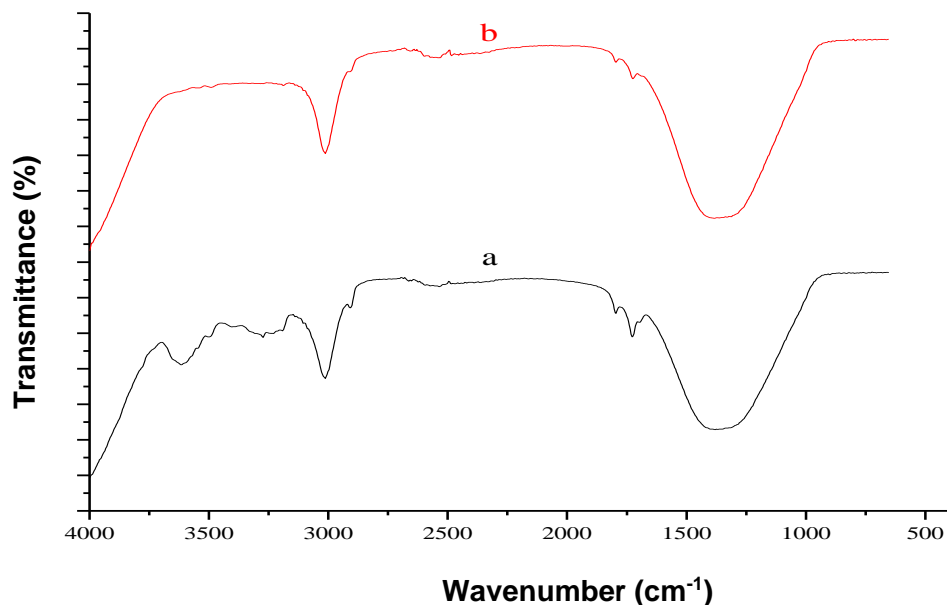
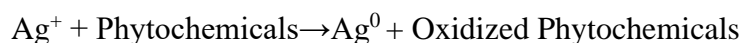


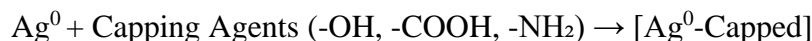
Fig. 10. FTIR measurement of (a) neem leaf extract and (b) AgNPs prepared from neem extract

Possible Mechanisms of Ag Capping

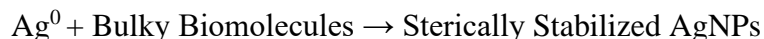
The synthesis and stabilization of silver nanoparticles (AgNPs) involve several key chemical interactions facilitated by phytochemicals. The reduction of silver ions (Ag^+) to metallic silver nanoparticles (Ag^0) is initiated by phytochemicals such as flavonoids, phenolics, and alkaloids, which donate electrons, leading to the following reaction:



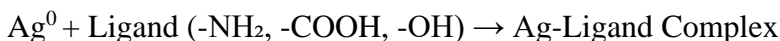
Once AgNPs are formed, they undergo stabilization through different mechanisms. Electrostatic stabilization occurs when negatively charged functional groups ($-\text{OH}$, $-\text{COOH}$, $-\text{NH}_2$) from capping agents bind to the AgNP surface, creating repulsive forces that prevent aggregation, as represented by:



Additionally, steric stabilization is achieved through the adsorption of bulky biomolecules, such as fatty acids and terpenoids, which form a protective layer around AgNPs, preventing them from clumping together. This process is described by:



Furthermore, chemical coordination enhances nanoparticle stability through ligand binding, where functional groups ($-\text{NH}_2$, $-\text{COOH}$, $-\text{OH}$) form coordination bonds with AgNPs, leading to:



These interactions collectively ensure the formation, stability, and functional properties of AgNPs, making them effective for various applications, including environmental monitoring and biomedicine.

Optimization Studies

Effects of neem concentration and time of reaction

The addition of silver nitrate (AgNO_3) to neem leaf extract caused the color to change from golden yellow to light brown, then dark brown, as seen previously in Fig. 2. The color change is caused by AgNPs produced by reducing silver salt. Neem leaf extract contains natural reducing agents, such as terpenoids and flavanones, which help reduce silver salt to AgNPs. According to Shankar *et al.* (2004), the golden-yellowish-brown color of AgNPs in aqueous solution is caused by surface plasmon vibrations. After about 60 min, the reaction mixture's color changed completely and did not change again. This shows that the silver in the reaction mixture was totally used up. The absorption spectrum is caused by strong surface plasmon resonance (SPR), which occurs when photons are resonantly absorbed by AgNPs. According to Amendola *et al.* (2010), the size and refractive index of the solution affect the reported absorption band of SPR. Figure 11 depicts the absorption spectra of AgNPs produced by the interaction of neem leaf extract with AgNO_3 within the wavelength range of 300 to 600 nm. The color of the neem leaf extract immediately changed after 10 min on addition of silver salt mixture. After 60 min, the solution's color became practically constant, suggesting the the completing reduction of all of the silver ions. When the concentration of neem leaf extract was less than 12.5 mg/mL, a faint absorbance band was seen. Increasing the concentration of the neem extract to 25 mg/mL resulted in a rapid increase in peak intensity, indicating improved generation of AgNPs. The strength of absorption increased consistently with increased concentration of neem extract (as illustrated in Fig. 11). Raising the content of the neem leaf extract caused the absorbance wavelength to shift towards reddish region (from 400 to 450 nm), confirming a rise in the AgNPs amount produced. In a report documented by Sneha *et al.* (2021), it was observed that when the extract percentage of *Cyclea peltata* leaf (CPL) in the production of AgNPs was varied between 5% and 20% w/v at 30 °C, 1 mM salt concentration, fixed pH for 6 h, the maximum yield was attained at 15% (w/v), and thereafter it was reduced with an increase in extract concentration.

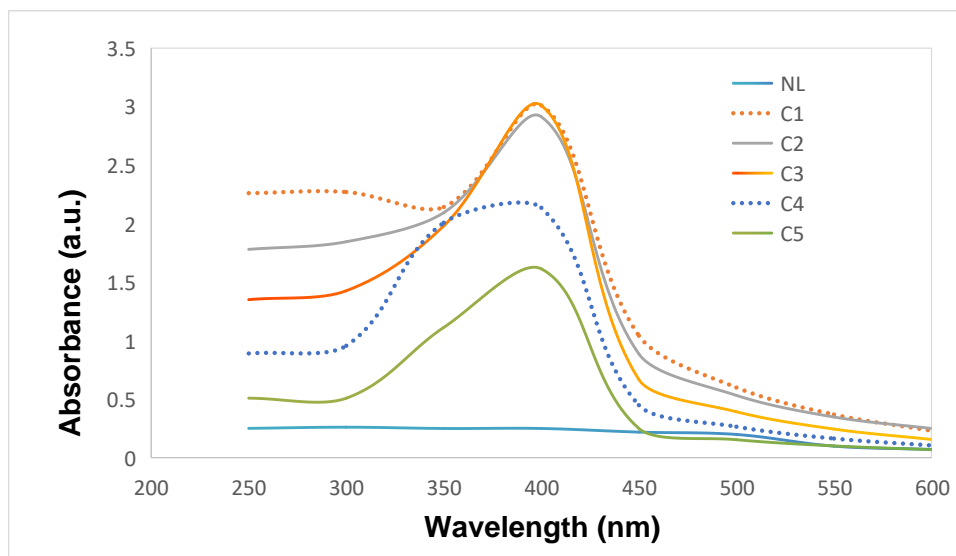


Fig. 11. UV-vis spectra of synthesized AgNPs at various plant extract concentrations at 1.0 mM AgNO_3 and for 1 h incubation (NL denotes neem leaf extract, C1, C2, C3, C4, and C5 stand for 100, 50, 25, 12.5, and 6.25 mg/mL)

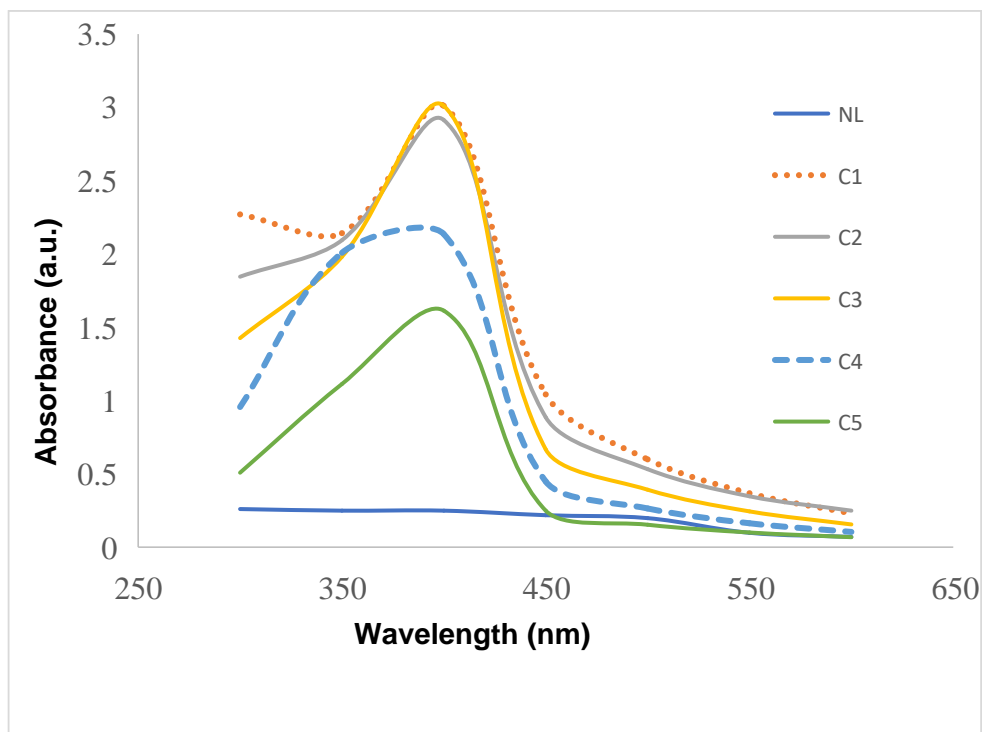


Fig. 12. UV-Vis spectra of synthesized AgNPs at various plant extract concentrations at 1.0 mM AgNO_3 and for 6 h incubation (NL denotes neem leaf extract, C1, C2, C3, C4, and C5 stand for 100, 50, 25, 12.5, and 6.25 mg/mL)

Effect of pH

The pH of the medium is necessary for the creation and stability of biogenic nanoparticles, as it changes the electrical charges of biomolecules, potentially altering the capping of nanoparticles formation (Priya *et al.* 2016). Figure 13 illustrates how pH affected the stability of nanoparticles as absorbance gradually increased with rising pH, thus, indicating a decrease in nanoparticles size and polydispersity (Qin *et al.* 2010). Absorbance gradually increased with rising pH, and the largest change in absorbance occurred between pH 8.0 and 10. As the pH of the solution increased, so did the peak of absorbance wavelength and intensity, as shown in Fig. 13. As the pH rose from 2.0 to 10.0, the absorbance maxima changed from 383 nm to 415 nm, and absorbance strength increases alongside the spectral shift. This implies that pH 10.0 is the optimal pH for AgNPs production from neem leaf extract, which is similar to the reports documented by Verma and Mehata (2016) that indicated an alkaline pH as the most suitable in producing AgNPs.

As the pH of the mixture rose, the peak wavelength shifted, indicating an increase in particle size. As particle diameter rises, the amount of energy needed to activate the surface plasma electrons is reduced, causing a shift in the peak of absorption to longer wavelengths. The elevated pH value increased the bio-accessibility of functional groups in the neem extract, leading to the formation of nanoparticles. Particles became unstable and aggregated when stored at elevated pH (< 10.5), as reported by Khalil *et al.* (2014), who observed that particle sizes increased as the pH of the mixture rose from 2.0 to 8.0 during the synthesis of AgNPs from olive leaf extract.

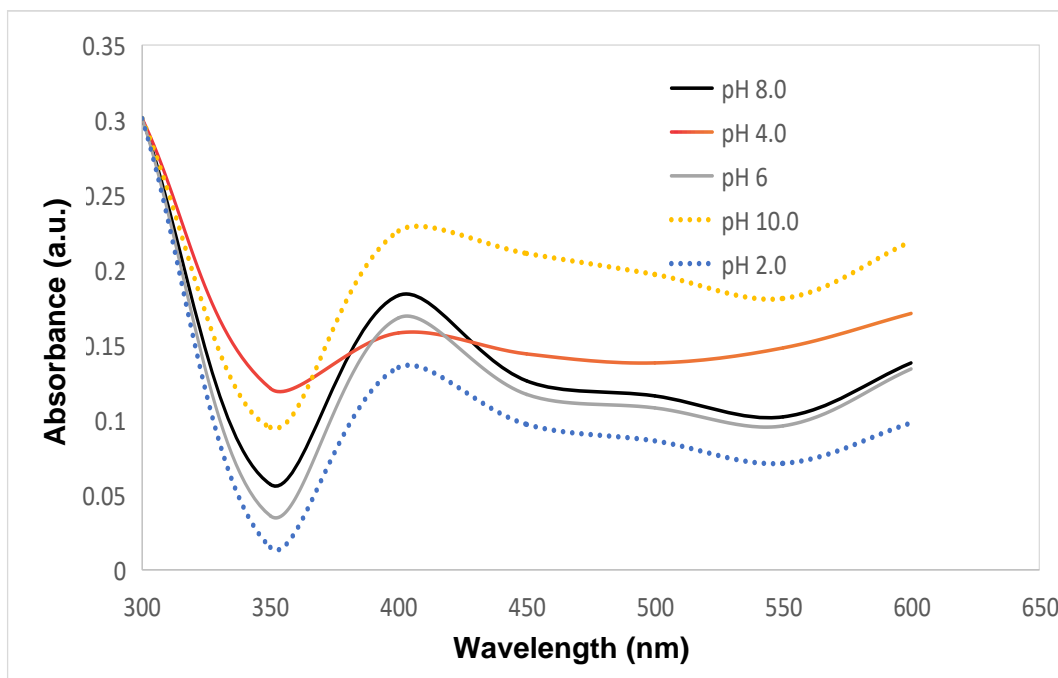


Fig. 13. Absorbance spectra of AgNPs at various pH (pH7.0 to 10.0)

Sneha *et al.* (2021) observed that the maximum pH in the production of CPL-AgNPs was pH 5, and this later declined when the pH was increased. It was argued that in acidic medium, the dissolution of AgNPs is high, which could facilitate the dissolution of nanoparticles due to smaller size but in basic medium, thermodynamic instability and high surface energy increased the size of the nanoparticles products, which results in agglomeration. Husam (2018) found that the synthesis of AgNPs using *Lawsonia inermis* extract achieved the highest color intensity at pH 9, while no reaction occurred at pH 3. Similarly, Muthuswamy *et al.* (2010) observed that low pH conditions favored the formation of larger nanoparticles, whereas higher pH conditions led to the production of smaller, well-dispersed nanoparticles. They explained that in acidic environments, aggregation of AgNPs was preferred over nucleation, resulting in larger particle sizes. In contrast, alkaline pH facilitated the presence of numerous functional groups that enhanced silver binding, leading to the formation of a greater number of smaller nanoparticles.

Pranlekha *et al.* (2017) also studied the effect of pH on AgNPs formation, observing that the SPR peaks shifted depending on the medium. In acidic conditions, SPR peaks were observed at shorter wavelengths (~330 nm), while in basic conditions, they shifted to longer wavelengths (414 nm), indicating a redshift. This shift was attributed to differences in the driving forces for AgNPs formation in acidic and basic media. In acidic conditions, a higher dissolution rate of AgNPs neutralized repulsive forces, maintaining nanoparticle dispersion and favoring the formation of smaller particles. Conversely, in basic conditions, sodium hydroxide dissociated to produce negatively charged hydroxide ions (OH^-), which enhanced the complete reduction of Ag^+ ions to AgNPs, resulting in larger particle sizes (Pranlekha *et al.* 2017).

Effect of Temperature

Figure 14 displays the absorbance bands of AgNPs at various temperatures (25 °C to 100 °C). As the temperature rose, silver salt reduction accelerated, resulting in a fast color shift in the solution. When the temperature rose from 25 to 100 °C, the peak absorbance wavelength moved towards blue shifts (400 to 395 nm) at 35 °C. The change in band maximum is caused by the location of SPR in AgNPs. Nanoparticle size was reduced as temperature increased, possibly due to increased reaction rates.

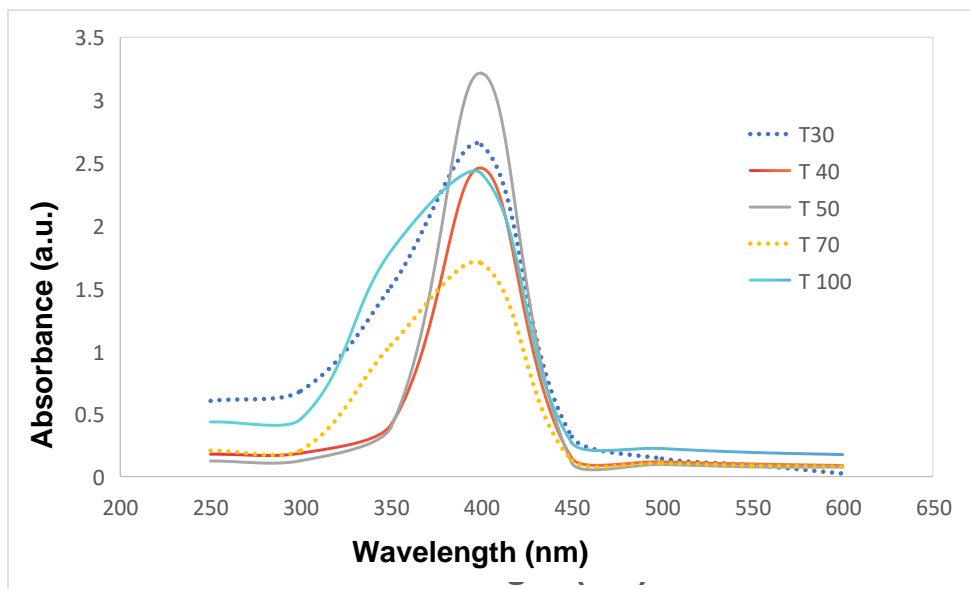


Fig. 14. Absorbance bands of AgNPs at various temperatures (25 to 100 °C)

Sneha *et al.* (2021) reported that the synthesis of CPL-AgNPs (silver nanoparticles from CPL extract) was most effective at a temperature of 35 °C, with reduced nanoparticle production observed at 40 °C. This decline was attributed to nanoparticle agglomeration, which resulted in increased particle size and altered shapes. Similarly, Husam (2018) investigated the effect of temperature on silver nanoparticle synthesis by analyzing UV-Vis spectra at 25, 35, and 45 °C. The study revealed that the rate of AgNPs formation increased with temperature, as indicated by a shift in wavelength. At lower temperatures, wavelengths were higher, corresponding to larger nanoparticle sizes, whereas at higher temperatures, wavelengths shifted to lower values, resulting in the formation of smaller nanoparticles.

Muthuswamy *et al.* (2010) also observed that higher temperatures enhanced both the productivity and the absolute value of the negative zeta potential of silver nanoparticles synthesized using *Curcuma longa* tuber powder and extract on cotton cloth. Additionally, they noted that the size of the nanoparticles tended to increase with rising temperatures, ranging from 20 to 60 °C.

Metal Ions Recognition and Selectivity of Neem Leaf AgNPs

The prepared AgNPs were examined for their ability to detect metal ions. When metal ions solutions (Pb^{2+} , Fe^{2+} , Cu^{2+} , Zn^{2+} , Cd^{2+} , Ni^{2+} , Mn^{2+} , and Ca^{2+}) were introduced to the prepared AgNPs solution, it resulted in a modest change in the strength of the surface plasmon resonance (LSPR) band, as shown in Fig. 15. Notably, the addition of these metal ions led to significant changes in the SPR band intensity, with the most

pronounced changes observed for Pb^{2+} and Cd^{2+} (Fig. 16). Several studies have used AuNPs as a colorimetric sensor to detect Pb^{2+} in aqueous media (Chen *et al.* 2011). This work focused on the shift of the SPR peak to a longer wavelength caused by Pb^{2+} binding on the surface of AgNPs, which led to the color change from golden yellow to brown. Other metals, such as Cu^{2+} , Zn^{2+} , Mg^{2+} , Ni^{2+} , Fe^{2+} , Cd^{2+} , Ca^{2+} , and Mn^{2+} , resulted in no important change on the nanoparticles' absorption spectra. Neem leaf synthesized AgNPs exhibit high selectivity for lead (Pb^{2+}) compared to other metals examined, indicating unique binding sites. The addition of organic functional groups, such as $-NH_2$, $-COOH$, and $-OH$, act as the stabilizing agent promoting the binding to the surface of AgNPs (Zangeneh *et al.* 2016).

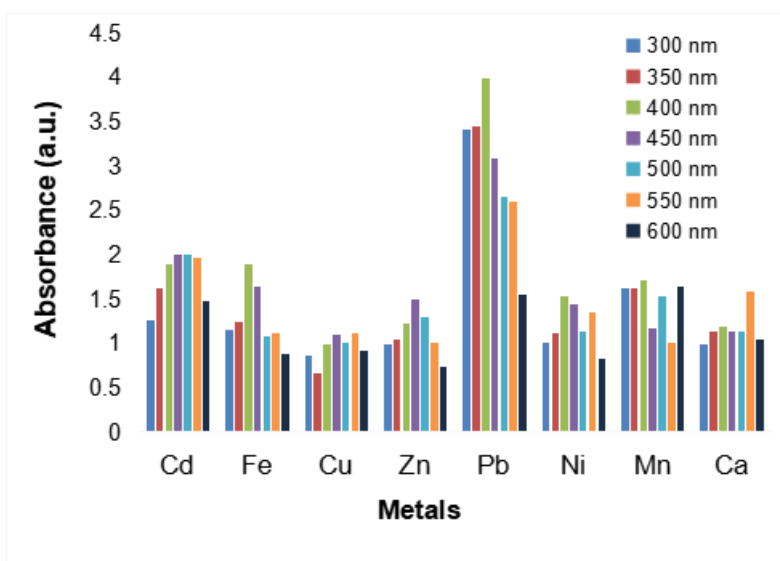


Fig. 15. Plots indicating the selectivity ability of AgNPs towards different metal ions

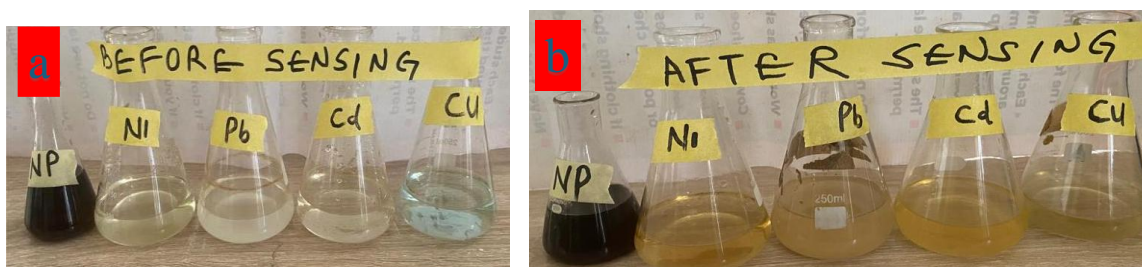


Fig. 16. Colors before (a) and after (b) sensing with AgNPs

CONCLUSIONS

This study utilized aqueous extracts of neem leaf as reducing and stabilizing agents to produce AgNPs. The process was optimized under different conditions of temperature, pH, time, and concentration of plant extract. The findings deduced are given below:

1. Silver nanoparticles (AgNPs) were synthesized *via* a cheap bio-reduction method from leaf extracts of *Azadirachta indica*.

2. Qualitative analysis of the leaf extract confirmed the presence of abundant biomolecules, which function as reducing, capping, and stabilizing agents in the synthesis of AgNPs.
3. The formation of AgNPs was confirmed by a strong surface plasmon resonance (SPR) band at 400 nm with an absorbance of 0.223 after 24 hours, as observed in the UV-Vis analysis.
4. The AgNPs demonstrated notable optical properties in response to the selected heavy metals, as evidenced by noticeable color changes upon the addition of metal ion solutions.
5. These findings demonstrate the successful synthesis of stable and well-defined AgNPs using the leaf extract and their potential as effective optical sensors for metal ion detection.

ACKNOWLEDGEMENTS

The authors express their gratitude to the Deanship of Scientific Research at Northern Border University, Arar, KSA, for funding this research work through the project number ““NBU-FFR-2025-2985-04””. We also appreciate Princess Nourah bint Abdulrahman University Researchers Supporting Project number (PNURSP2025R65), Princess Nourah bint Abdulrahman University, Riyadh, Saudi Arabia.

Competing Interests

No competing interest exists

REFERENCES CITED

- Ahmed, R. H., and Mustafa, D. E. (2020). “Green synthesis of silver nanoparticles mediated by traditionally used medicinal plants in Sudan,” *International Nano Letters* 10, 1-14. DOI: 10.1007/s40089-019-00291-9
- Akinwekomi, V., Maree, J., Zvinowanda, C., and Masindi, V. (2017). “Synthesis of magnetite from iron-rich mine water using sodium carbonate,” *Journal of Environmental Chemical Engineering* 5(3), 2699-2707. DOI: 10.1016/j.jece.2017.05.025
- Alberti, G., Zanoni, C., Magnaghi, L.R., and Biesuz, R. (2021). “Gold and silver nanoparticle-based colorimetric sensors: New trends and applications,” *Chemosensors* 9, article 305. DOI: 10.3390/chemosensors9110305
- Ali, H., Khan, E., and Sajad, M. A. (2013). “Phytoremediation of heavy metals— Concepts and applications,” *Chemosphere* 91(7), 869-881. DOI: 10.1016/j.chemosphere.2013.01.075
- Amendola, V., Bakr, O. M., and Stellacci, F. (2010). “A study of the surface plasmon resonance of silver nanoparticles by the discrete dipole approximation method: Effect of shape, size, structure, and assembly,” *Plasmonics* 5, 85-97. DOI: 10.1016/j.jece.2017.05.025
- Annadhasan, M., Muthukumarasamyvel, T., Sankar Babu, V., and Rajendiran, N. (2014). “Green synthesized silver and gold nanoparticles for colorimetric detection of Hg²⁺,

- Pb²⁺, and Mn²⁺ in aqueous medium,” *ACS Sustainable Chemistry and Engineering* 2, 887-896. DOI:10.1021/sc400500z
- Babel, S., and Kurniawan, T.A. (2003). “Low-cost adsorbents for heavy metals uptake from contaminated water: A review,” *Journal of hazardous materials* 97(1-3), 219-243. Doi.org/10.1016/S0304-3894(02)00263-7
- Badhiwala, J. H., Nassiri, F., Alhazzani, W., Selim, M. H., Farrokhyar, F., Spears, J., Kulkarni, A. V., Singh, S., Alqahtani, A., and Rochweg, B. (2015). “Endovascular thrombectomy for acute ischemic stroke: A meta-analysis,” *Jama* 314(17), 1832-1843. DOI: 10.1001/jama.2015.13767
- Baruah, S., Najam, K. M., and Dutta, J. (2016). “Perspectives and applications of nanotechnology in water treatment,” *Environmental Chemistry Letters* 14, 1-14. DOI: 10.1007/s10311-015-0542-2
- Bhat, R. S., Almusallam, J., Al Daihan, S., and Al-Dbass, A. (2019). “Biosynthesis of silver nanoparticles using *Azadirachta indica* leaves: Characterisation and impact on *staphylococcus aureus* growth and glutathione-S-transferase activity,” *IET Nanobiotechnology* 13(5), 42-46. DOI: 10.1049/iet-nbt.2018.5133
- Chen, X., Zu, Y., Xie, H., Kemas, A. M., and Gao, Z. (2011). “Coordination of mercury (II) to gold nanoparticle associated nitrotriazole towards sensitive colorimetric detection of mercuric ion with a tunable dynamic range,” *Analyst* 136, 1690-1696. DOI: 10.1039/C0AN00903B
- Choi, Y., Kang, S., Cha, S.-H., Kim, H.-S., Song, K., Lee, Y. J., Kim, K., Kim, Y. S., Cho, S., and Park, Y. (2018). “Platycodon saponins from *Platycodi radix* (*Platycodon grandiflorum*) for the green synthesis of gold and silver nanoparticles,” *Nanoscale Research Letters* 13, 1-10.
- Daşbaşı, T., Saçmacı, Ş., Çankaya, N., and Soykan, C. (2016). “A new synthesis, characterization and application chelating resin for determination of some trace metals in honey samples by FAAS,” *Food Chemistry* 203, 283-291. DOI: 10.1016/j.foodchem.2016.02.078
- Dash, S. P., Dixit, S., and Sahoo, S. (2017). “Phytochemical and biochemical characterizations from leaf extracts from *Azadirachta indica*: An important medicinal plant,” *Biochem Anal Biochem* 6, 2161-1009. DOI: 10.4172/2161-1009.1000323
- Dhand, V., Soumya, L., Bharadwaj, S., Chakra, S., Bhatt, D., and Sreedhar, B. (2016). “Green synthesis of silver nanoparticles using *Coffea arabica* seed extract and its antibacterial activity,” *Materials Science and Engineering: C* 58, 36-43. DOI: 10.1016/j.msec.2015.08.018.
- Du, J., Jiang, L., Shao, Q., Liu, X., Marks, R. S., Ma, J., and Chen, X. (2012). “Colorimetric detection of mercury ions based on plasmonic nanoparticles,” *Small* 9(9-10), 1467-1481. DOI: 10.1002/sml.201200811
- Duodu, G. O., Goonetilleke, A., and Ayoko, G. A. (2016). “Comparison of pollution indices for the assessment of heavy metal in Brisbane River sediment,” *Environmental Pollution* 219, 1077-1091. DOI: 10.1016/j.envpol.2016.09.008
- Fu, F., and Wang, Q. (2011). “Removal of heavy metal ions from wastewaters: A review,” *Journal of Environmental Management* 92(3), 407-418. DOI: 10.1016/j.jenvman.2010.11.011
- Hills, G., Lau, C., Wright, A., Fuller, S., Bishop, M. D., Srimani, T., Kanhaiya, P., Ho, R., Amer, A., and Stein, Y. (2019). “Modern microprocessor built from complementary carbon nanotube transistors,” *Nature* 572, 595-602. DOI: 10.1038/s41586-019-1493-8

- Hou, S., Yuan, L., Jin, P., Ding, B., Qin, N., Li, L., Liu, X., Wu, Z., Zhao, G., and Deng, Y. (2013). "A clinical study of the effects of lead poisoning on the intelligence and neurobehavioral abilities of children," *Theoretical Biology and Medical Modelling* 10, 1-9. DOI: 10.1186/1742-4682-10-13
- Husam, M. K. (2018). "The effect of pH, temperature on the green synthesis and biochemical activities of silver nanoparticles from *Lawsonia inermis* extract," *J. Pharm. Sci. & Res.* 10(8), 2022-2026.
- Jebril, S., Jenana, R. K. B., and Dridi, C. (2020). "Green synthesis of silver nanoparticles using *Melia azedarach* leaf extract and their antifungal activities: In vitro and in vivo," *Materials Chemistry and Physics* 248, article 22898. DOI: 10.1016/j.matchemphys.2020.122898
- Kaji, M. (2015). "Itai-itai disease: Lessons for the way to environmental regeneration," in: Y. Fujigaki (ed.), *Lessons from Fukushima*," Springer, Cham. DOI: 10.1007/978-3-319-15353-7_7.
- Khalil, M. M., Ismail, E. H., El-Baghdady, K. Z., and Mohamed, D. (2014). "Green synthesis of silver nanoparticles using olive leaf extract and its antibacterial activity," *Arabian Journal of Chemistry* 7(6), 1131-1139. DOI: 10.1016/j.arabjc.2013.04.007
- Koduru, J. R., Kailasa, S. K., Bhamore, J. R., Kim, K.-H., Dutta, T., and Vellingiri, K. (2018). "Phytochemical-assisted synthetic approaches for silver nanoparticles: Antimicrobial applications: A review," *Advances in Colloid and Interface Science* 256, 326-339. DOI: 10.1016/j.cis.2018.03.001
- Krishnaraj, C., Jagan, E., Rajasekar, S., Selvakumar, P., Kalaichelvan, P., and Mohan, N. (2010). "Synthesis of silver nanoparticles using *Acalypha indica* leaf extracts and its antibacterial activity against water borne pathogens," *Colloids and Surfaces B: Biointerfaces* 76(1), 50-56. DOI: 10.1016/j.colsurfb.2009.10.008
- Kumari, S. A., Patlolla, A. K., and Madhusudhanachary, P. (2022). "Biosynthesis of silver nanoparticles using *Azadirachta indica* and their antioxidant and anticancer effects in cell lines," *Micromachines* 13, article 1416. DOI: 10.3390/mi13091416
- Liao, R., Xu, J. and Umemura, K. (2016). "Low density sugarcane bagasse particleboard bonded with citric acid and sucrose: Effect of board density and additive content," *BioResources* 11(1), 2174-2185.
- Magagane, N., Masindi, V., Ramakokovhu, M. M., Shongwe, M. B. and Muedi, K. L. (2019). "Facile thermal activation of non-reactive cryptocrystalline magnesite and its application on the treatment of acid mine drainage," *Journal of Environmental Management* 236, 499-509. DOI: 10.1016/j.jenvman.2019.02.030
- Maity, M., Bera, K., Pal, U., Khamaru, K., and Maiti, N. C. (2018). "Sensing of Fe(III) ion via modulation of redox potential on biliverdin protected silver nanosurface," *ACS Applied Nano Materials*. DOI: 10.1021/acsanm.8b01311
- Meenambal, M., Pughalendy, K., Vasantharaja, C., Prapakaran, S., and Vijayan, P. (2012). "Phytochemical information from FTIR and GC-MS studies of methol extract of *Delonix elat* leaves," *International Journal of Chemical and Analytical Science* 3, 1446-1448.
- Mitra, S., Kandambeth, S., Biswal, B. P., Khayum, M. A., Choudhury, C. K., Mehta, M., Kaur, G., Banerjee, S., Prabhune, A., and Verma, S. (2016). "Self-exfoliated guanidinium-based ionic covalent organic nanosheets (iCONs)," *Journal of the American Chemical Society* 138, 2823-2828. DOI: 10.1021/jacs.5b13533. Epub 2016 Feb 19

- Mudhafar, M., Zainol, I., Jaafar, C. N., and Alsailawi, H. A. (2020). "Phytochemical screening and quantitative analysis of *Azadirachta indica* leaf extracts," *Journal of Medicinal Plants Research*, 14(4), 123-130.
- Muthuswamy, S., Krishnamurthy, S., and Yeoung-Sang, Y. (2010). "Immobilization of silver nanoparticles synthesized using *Curcuma longa* tuber powder and extract on cotton cloth for bactericidal activity," *Bioresource Technology* 101, 7958-7965. DOI: 10.1016/j.biortech.2010.05.0
- Nasrollahzadeh, M., Sajadi, S. M., Sajjadi, M., and Issaabadi, Z. (2019). "An introduction to nanotechnology," *Interface Science and Technology*, 1-27. DOI: 10.1016/B978-0-12-813586-0.00001-8
- Pranlekha, T., Kriengkri, T., and Chatchawa, W. (2017). "Flexible room-temperature resistive humidity sensor based on silver nanoparticles," *Mater. Res. Express* 4, article 085038. DOI: 10.1088/2053-1591/aa85b6
- Priya, R. S., Geetha, D., and Ramesh, P. (2016). "Antioxidant activity of chemically synthesized AgNPs and biosynthesized *Pongamia pinnata* leaf extract mediated AgNPs—A comparative study," *Ecotoxicology and Environmental Safety* 134, 308-318. DOI: 10.1016/j.ecoenv.2015.07.037
- Qin, Y., Ji, X., Jing, J., Liu, H., Wu, H., and Yang, W. (2010). "Size control over spherical silver nanoparticles by ascorbic acid reduction," *Colloids and Surfaces A: Physicochemical and Engineering Aspects* 372(1-3), 172-176. DOI: 10.1016/j.colsurfa.2010.10.013
- Raja, P. B., Rahim, A. A., Qureshi, A. K., and Awang, K. (2014). "Green synthesis of silver nanoparticles using tannins," *Materials Science-Poland* 32, 408-413. DOI: 10.2478/s13536-014-0204-2
- Shankar, S. S., Rai, A., Ahmad, A., and Sastry, M. (2004). "Rapid synthesis of Au, Ag, and bimetallic Au core–Ag shell nanoparticles using Neem (*Azadirachta indica*) leaf broth," *Journal of Colloid and Interface Science* 275(2), 496-502. DOI: 10.1016/j.jcis.2004.03.003
- Sneha, N., Manjunatha, K. B., Louella, C. G., Vaman, C. R., and Shyama, P. S. (2021). "Investigation of nonlinear optical properties of AgNPs synthesized using *Cyclea peltata* leaf extract post OVAT optimization," *BioNanoScience* 11(3), 884-892. DOI: 10.1007/s12668-021-00875-w
- Singh, A., Gaud, B. and Jaybhaye, S. (2020). "Optimization of synthesis parameters of silver nanoparticles and its antimicrobial activity," *Materials Science for Energy Technologies* 3, 232-236. DOI: 10.1016/j.mset.2019.08.004
- Sun, H., Brocato, J., and Costa, M. (2015). "Oral chromium exposure and toxicity," *Current Environmental Health Reports* 2, 295-303. DOI: 10.1007/s40572-015-0054-z
- Tabassum, T., Farooq, M., Ahmad, R., Zohaib, A., and Wahid, A. (2017). "Seed priming and transgenerational drought memory improves tolerance against salt stress in bread wheat," *Plant Physiology and Biochemistry* 118, 362-369. DOI: 10.1016/j.plaphy.2017.07.007
- Varela, J. P., Valente, A. J., and Durães, L. (2019). "Assessment of heavy metal pollution from anthropogenic activities and remediation strategies: A review," *Journal of Environmental Management* 246, 101-118. DOI: 10.1016/j.jenvman.2019.05.126
- Velusamy, P., Das, J., Pachaiappan, R., Vaseeharan, B., and Pandian, K. (2015). "Greener approach for synthesis of antibacterial silver nanoparticles using aqueous solution of neem gum (*Azadirachta indica* L.)," *Industrial crops and Products* 66, 103-109. DOI: 10.1016/j.indcrop.2014.12.042

- Verma, A. and Mehata, M. S. (2016). “Controllable synthesis of silver nanoparticles using Neem leaves and their antimicrobial activity,” *Journal of radiation Research and Applied Sciences* 9(1), 109-115. DOI: 10.1016/j.jrras.2015.11.001
- Wang, Q., Xie, Z. and Li, F. (2015). “Using ensemble models to identify and apportion heavy metal pollution sources in agricultural soils on a local scale,” *Environmental Pollution* 206, 227-235. DOI: 10.1016/j.envpol.2015.06.040
- Wu, Y., Pang, H., Liu, Y., Wang, X., Yu, S., Fu, D., Chen, J., and Wang, X. (2019). “Environmental remediation of heavy metal ions by novel-nanomaterials: A review,” *Environmental Pollution* 246, 608-620. DOI: 10.1016/j.envpol.2018.12.076
- Yaqoob, A. A., and Ibrahim, M. N. M. (2019). “A review article of nanoparticles; Synthetic approaches and wastewater treatment methods,” *International Research Journal of Engineering and Technology* 6(3), article 2395.
- Zangeneh, K., Pandikumar, A., Jayabal, S., Ramaraj, R., Lim, H. N., Ong, B. H., Bien, C. S. D., Kee, Y. Y., and Huang, N. M. (2016). “Amalgamation based optical and colorimetric sensing of mercury (II) ions with silver@ graphene oxide nanocomposite materials,” *Microchimica Acta* 183, 369-377. DOI: 10.1007/s00604-015-1658-6
- Zwolak, A., Sarzyńska, M., Szpyrka, E., and Stawarczyk, K. (2019). “Sources of soil pollution by heavy metals and their accumulation in vegetables: A review,” *Water, Air, & Soil Pollution* 230, article 164. DOI: 10.1007/s11270-019-4221-y

Article submitted: November 23, 2024; Peer review completed: January 4, 2025; Revised version received: February 25, 2025; Accepted: February 27, 2025; Published: March 13, 2025.

DOI: 10.15376/biores.20.2.3342-3366